Supporting information for

Unique structural features of mule deer prion protein provide insights into chronic wasting disease

Urška Slapšak[1#], Giulia Salzano[2#], Gregor Ilc[1,3], Gabriele Giachin[2,4], Jifeng Bian[5,6], Glenn Telling[5,6], Giuseppe Legname[2,7], Janez Plavec[1,3,8*]*

[1]Slovenian NMR Centre, National Institute of Chemistry, SI-1000 Ljubljana, Slovenia; [2]Laboratory of Prion Biology, Department of Neuroscience, Scuola Internazionale Superiore di Studi Avanzati (SISSA), Via Bonomea 265, Trieste I-34136, Italy,

[3]EN-FIST Centre of Excellence, SI-1000 Ljubljana, Slovenia,

[4]Structural Biology Group, European Synchrotron Radiation Facility (ESRF), 38000-Grenoble, France;

[5]Prion Research Center (PRC), Colorado State University, Fort Collins, CO 80525, USA; [6]Department of Microbiology, Immunology and Pathology, Colorado State University, Fort Collins, CO 80525, USA;

[7]ELETTRA -Sincrotrone Trieste S.C.p.A, Trieste, 34149, Italy

[8]Department of Chemistry and Biochemistry, Faculty of Chemistry and Chemical Technology, University of Ljubljana, SI-1000 Ljubljana, Slovenia

[#]These authors equally contributed to this work.

[*] To whom correspondence should be addressed: Janez Plavec: Slovenian NMR Centre, National Institute of Chemistry, SI-1000 Ljubljana, Slovenia;
janez.plavec@ki.si; TEL +386 47 60 353; and
Giuseppe Legname: Laboratory of Prion Biology, Department of Neuroscience, Scuola Internazionale Superiore di Studi Avanzati (SISSA), Via Bonomea 265, Trieste I-34136, Italy;
legname@sissa.it; TEL +39 040 3787 715, FAX +39 040 3787 702

Table S1. Local backbone RMSD values that represent overlap of three-residue segment centred at each residue in the sequence of overlaid mdPrP, wtdPrP and ePrP structures.[a]

aa residue[b]	RMSD (Å)	aa residue	RMSD (Å)	aa residue	RMSD (Å)
Leu[128]	3.49	Asn[162]	0.69	Thr[196]	3.48
Gly[129]	3.29	Gln[163]	0.74	Lys[197]	3.52
Gly[130]	3.10	Val[164]	0.64	Gly[198]	3.14
Tyr[131]	1.39	Tyr[165]	0.51	Glu[199]	2.91
Met[132]	0.63	Tyr[166]	0.38	Asn[200]	4.02
Leu[133]	0.74	Arg[167]	0.73	Phe[201]	4.20
Gly[134]	0.71	Pro[168]	1.02	Thr[202]	3.64
Ser[135]	1.34	Val[169]	1.22	Glu[203]	3.35
Ala[136]	1.68	Asp[170]	1.86	Thr[204]	2.51
Met[137]	1.78	Gln[171]	1.58	Asp[205]	2.20
Ser[138]	2.41	Tyr[172]	1.73	Ile[206]	2.27
Arg[139]	2.14	Asn[173]	1.97	Lys[207]	1.99
Pro[140]	1.68	Asn[174]	1.15	Met[208]	1.28
Leu[141]	1.62	Gln[175]	1.24	Met[209]	1.06
Ile[142]	1.41	Asn[176]	1.32	Glu[210]	1.13
His[143]	1.52	Thr[177]	1.19	Arg[211]	0.83
Phe[144]	2.17	Phe[178]	1.10	Val[212]	0.77
Gly[145]	2.37	Val[179]	0.86	Val[213]	0.66
Asn[146]	2.42	His[180]	1.28	Glu[214]	0.68
Asp[147]	3.62	Asp[181]	1.26	Gln[215]	0.77
Tyr[148]	2.86	Cys[182]	0.81	Met[216]	0.66
Glu[149]	1.65	Val[183]	0.90	Cys[217]	0.76
Asp[150]	2.05	Asn[184]	0.75	Ile[218]	0.73
Arg[151]	2.22	Ile[185]	0.59	Thr[219]	0.84
Tyr[152]	1.25	Thr[186]	0.48	Gln[220]	1.02
Tyr[153]	0.79	Val[187]	0.76	Tyr[221]	1.01
Arg[154]	1.42	Lys[188]	0.63	Gln[222]	0.63
Glu[155]	0.92	Gln[189]	0.77	Arg[223]	0.86
Asn[156]	1.02	His[190]	1.48	Glu[224]	1.00
Met[157]	1.40	Thr[191]	1.61	Ser[225]	0.89
Tyr[158]	2.29	Val[192]	1.97	Gln[226]	1.24
Arg[159]	2.02	Thr[193]	2.23	Ala[227]	2.53
Tyr[160]	1.60	Thr[194]	2.77	Tyr[228]	2.39
Pro[161]	1.01	Thr[195]	3.18		

[a] RMSD values have been calculated with program CHIMERA. We superimposed three structures of mdPrP, ePrP and wtdPrP that have lowest energies in NMR ensemble first, and then we calculated the backbone RMSD values per residue of superimposed structures.

[b] Residue numbering is based on mdPrP amino acid sequence. RMSD values are showed for residues from 128 to 228.

Table S2. Distances between C-atoms of selected amino acid residues of mdPrP, wtdPrP and ePrP structures.[a]

distance	**mdPrP** (Å)	**wtdPrP** (Å)	**ePrP** (Å)
$Leu^{128}C_{\delta1}$-$Ile^{185}C_{\delta1}$	3.8 ± 0.1	9.4	8.5 ± 0.3
$Tyr^{131}C_{\zeta}$-$Ile^{185}C_{\delta1}$	6.3 ± 0.1	3.2	5.1 ± 0.3
$Phe^{144}C_{\zeta}$-$Tyr^{153}C_{\zeta}$	6.1 ± 0.2	5.2	4.7 ± 0.6
$Tyr^{148}C_{\zeta}$-$Tyr^{152}C_{\zeta}$	3.9 ± 0.2	6.2	9.0 ± 1.6
$Tyr^{148}C_{\zeta}$-$Thr^{202}C_{\gamma2}$	8.1 ± 0.4	16.4	8.3 ± 1.7
$Tyr^{148}C_{\zeta}$-$Thr^{204}C_{\gamma2}$	5.2 ± 0.4	12.3	6.7 ± 1.1
$Tyr^{152}C_{\zeta}$-$Thr^{202}C_{\gamma2}$	5.2 ± 0.3	8.7	4.4 ± 1.0
$Tyr^{152}C_{\zeta}$-$Thr^{204}C_{\gamma2}$	5.1 ± 0.4	6.2	4.8 ± 0.8
$Val^{169}C_{\beta}$-$Ser^{225}C_{\beta}$	5.5 ± 0.2	6.1	5.5 ± 0.4
$Val^{169}C_{\beta}$-$Tyr^{228}C_{\zeta}$	4.3 ± 0.3	6.7	7.5 ± 0.6
$Tyr^{221}C_{\zeta}$-$Ser^{225}C_{\beta}$	4.3 ± 0.3	5.0	4.9 ± 0.5
$Ser^{225}C_{\beta}$-$Tyr^{228}C_{\zeta}$	8.5 ± 0.2	8.7	7.8 ± 0.3
$Ser^{225}C_{\beta}$-$Tyr^{229}C_{\zeta}$	5.0 ± 0.2	NA[b]	10.2 ± 0.4

[a] Reported distances are average values obtained from coordinates of structural ensemble for mdPrP (PDB id 6FNV) and ePrP (PDB id 1XYW) that were determined by NMR, and wtdPrP (PDB id 4YXH) determined by X-ray crystallography. Standard deviations are reported for the ensembles of 20 lowest energies structures of mdPrP and ePrP that have been determined by NMR.

[b] NA – not applicable

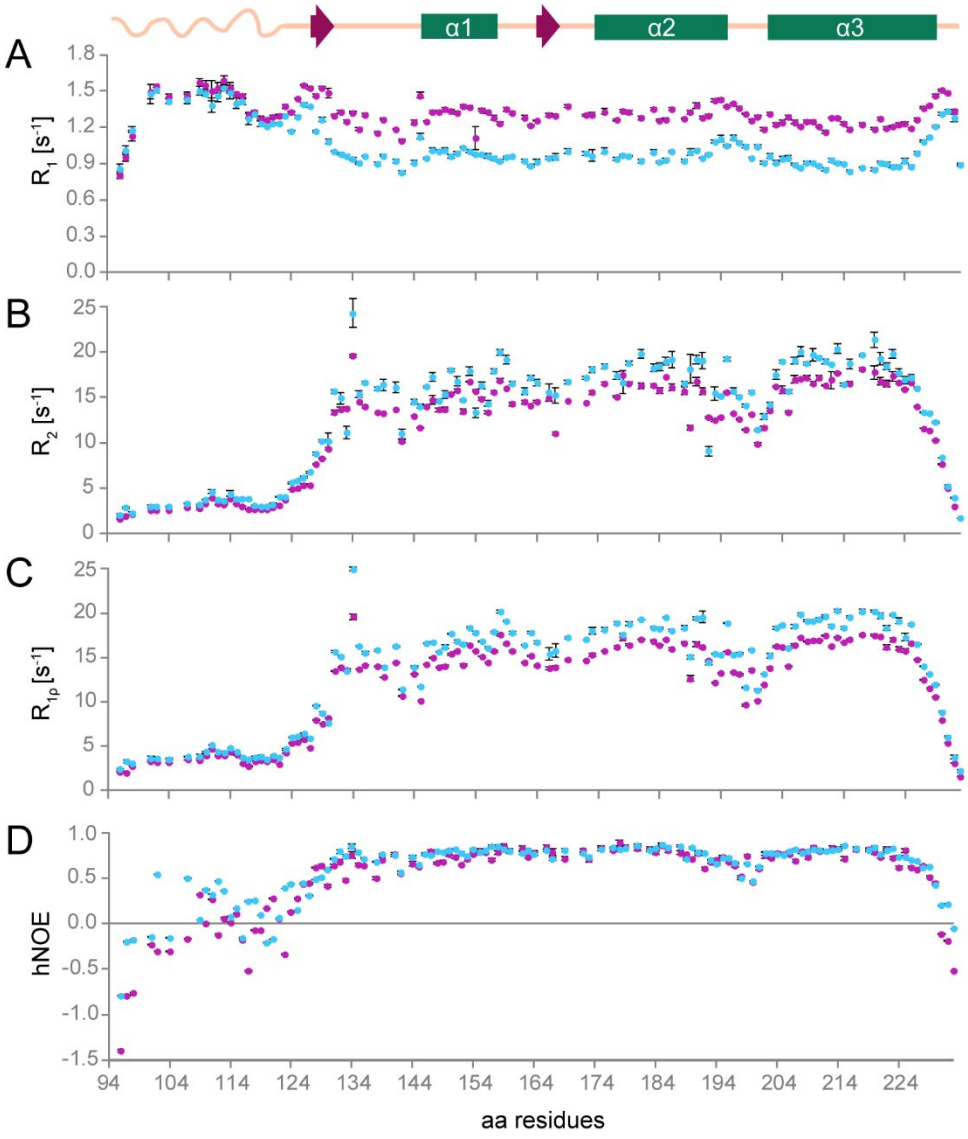

Figure S1. ^{15}N amide backbone relaxation rates and hNOE of mdPrP. The same as Figure 4 at manuscript with included error bars. A) ^{15}N longitudinal ($R_1=1/T_1$), B) transverse ($R_2=1/T_2$), C) spin-lattice relaxation rates in the rotation frame ($R_{1\rho}=1/T_{1\rho}$) and D) hNOE at 298 K at magnetic field of 14.1 (magenta) and 18.8 T (blue). A schematic presentation of secondary structure elements of mdPrP is at the top of the figure. The error bars represent standard deviation of R_1 (A), R_2 (B) and $R_{1\rho}$ (C) relaxation rates and hNOE values (D).

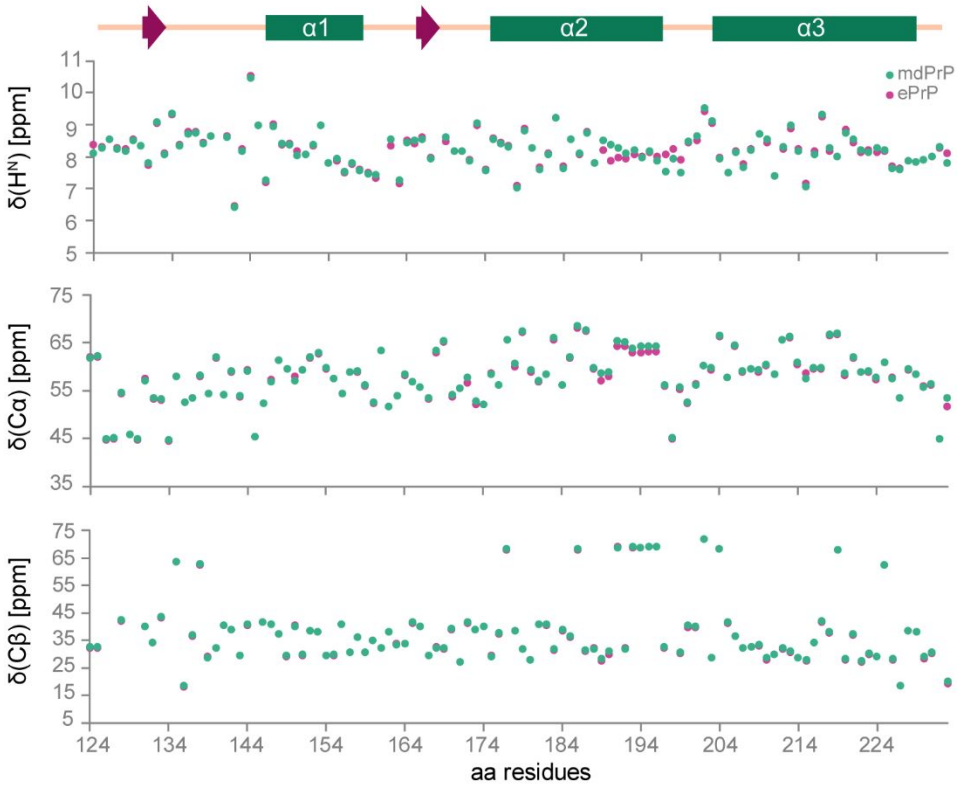

Figure S2. Chemical shifts of H^N, Cα and Cβ atoms of mdPrP (green) and ePrP (magenta) structures (residues from 124 to 233). Data for ePrP was reported earlier (BMRB id 6383).

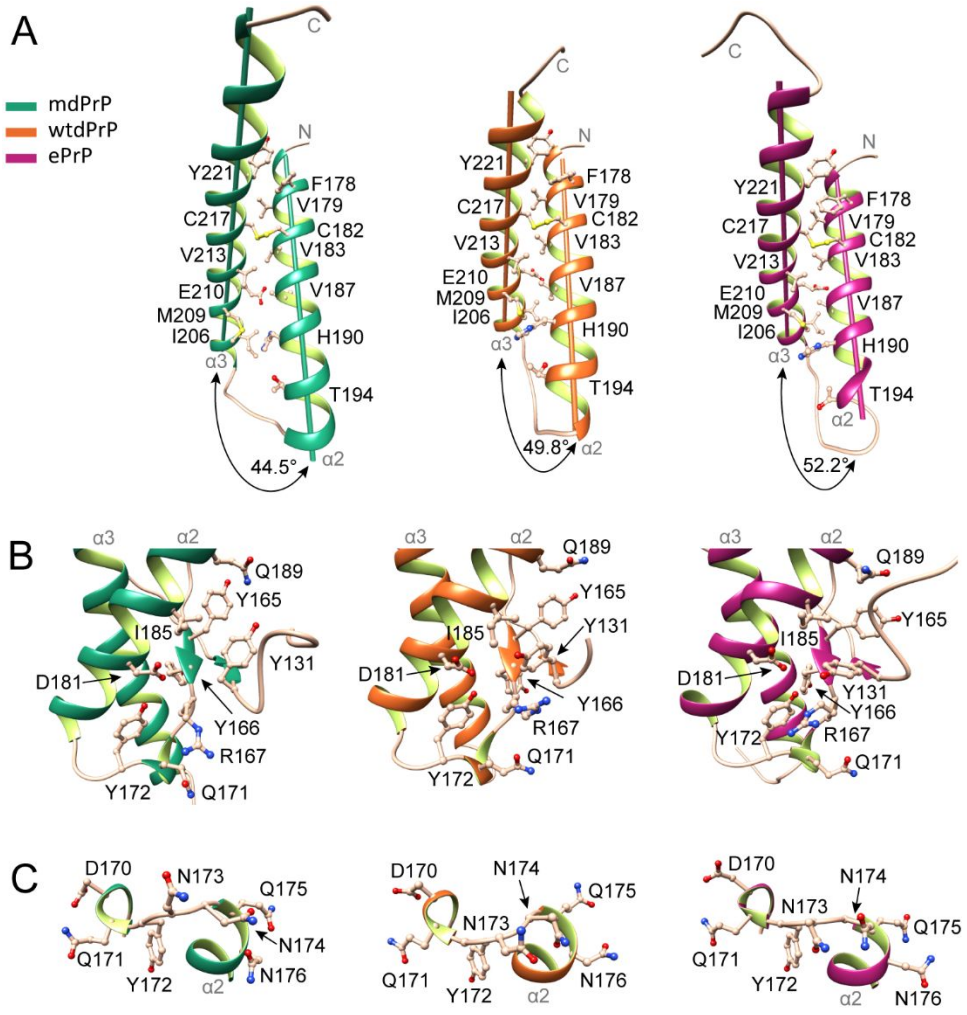

Figure S3. Structural diversity of mdPrP, wtdPrP and ePrP. Structure of mdPrP is shown in green, wtdPrP in orange and ePrP in magenta. Marked amino acid residues are presented as a ball-and-stick. A) α2 and α3 helices of mdPrP, wtdPrP and ePrP structures. B) Arrangements of amino acid residues that are in the proximity of Tyr^{131}. C) Orientation of Asp^{170}, Gln^{171}, Tyr^{172}, Asn^{173}, Ans^{174}, Gln^{175} and Ans^{176} in β2-α2 loop.

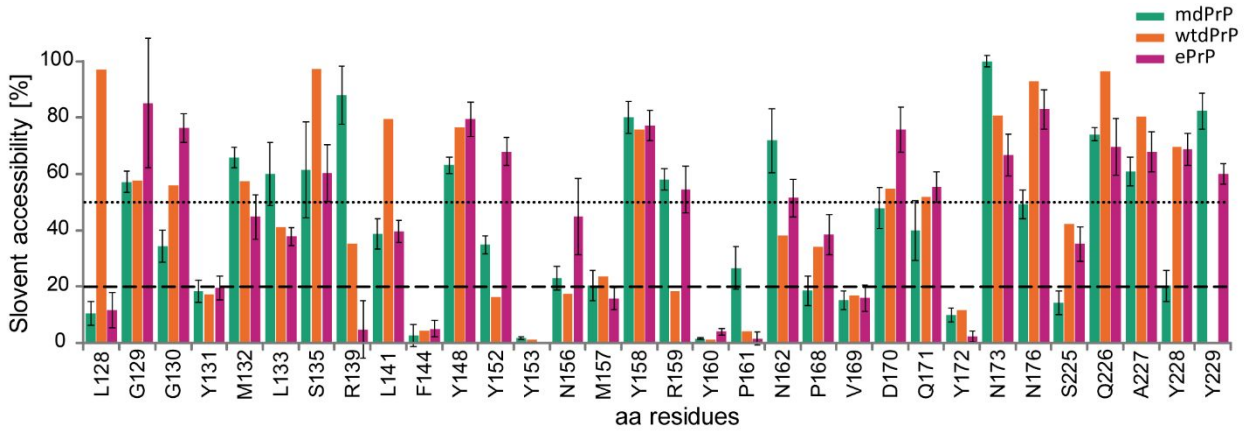

Figure S4. Solvent accessibility of selected amino acid residues of mdPrP, wtdPrP and ePrP. Hatched and dotted lines at 20% and 50% indicate limits of amino acid residue accessibility to the solvent (>50%) or burial in solvent inaccessible regions (<20%). Standard deviations are reported and have been calculated for the family of 20 lowest energies structures of mdPrP and ePrP that have been determined by NMR.